Cardiovascular Research (2016) **109**, 174–184
doi:10.1093/cvr/cvv254

Nitrated fatty acids suppress angiotensin II-mediated fibrotic remodelling and atrial fibrillation

Tanja K. Rudolph[1†], Thorben Ravekes[1†], Anna Klinke[1,2], Kai Friedrichs[1], Martin Mollenhauer[1], Michaela Pekarova[3], Gabriela Ambrozova[3], Hana Martiskova[3], Jatinder-Jit Kaur[4], Bianca Matthes[4], Alex Schwoerer[5,6], Steven R. Woodcock[7], Lukas Kubala[2,3], Bruce A. Freeman[7], Stephan Baldus[1], and Volker Rudolph[1]*

[1]Department of Cardiology, University Heart Center Cologne, University of Cologne, Kerpener Str. 62, 50937 Cologne, Germany; [2]International Clinical Research Center—Center of Biomolecular and Cellular Engineering, St Anne's University Hospital Brno, Brno, Czech Republic; [3]Institute of Biophysics, Academy of Sciences of the Czech Republic, v. v. I, Brno, Czech Republic; [4]Department of Cardiology, University Heart Center Hamburg, University Hospital Eppendorf, Hamburg, Germany; [5]Department of Cellular and Integrative Physiology, University Medical Center Hamburg Eppendorf, Hamburg, Germany; [6]DZHK (German Centre for Cardiovascular Research)–Hamburg/Kiel/Luebeck, Hamburg, Germany; and [7]Department of Pharmacology and Chemical Biology, University of Pittsburgh, Pittsburgh, PA, USA

Received 24 April 2015; revised 12 October 2015; accepted 6 November 2015; online publish-ahead-of-print 23 November 2015

Time for primary review: 20 days

Aim Atrial fibrosis, one of the most striking features in the pathology of atrial fibrillation (AF), is promoted by local and systemic inflammation. Electrophilic fatty acid nitroalkenes, endogenously generated by both metabolic and inflammatory reactions, are anti-inflammatory mediators that in synthetic form may be useful as drug candidates. Herein we investigate whether an exemplary nitro-fatty acid can limit atrial fibrosis and AF.

Methods and results Wild-type C57BL6/J mice were treated for 2 weeks with angiotensin II (AngII) and vehicle or nitro-oleic acid (10-nitro-octadec-9-enoic acid, OA-NO_2, 6 mg/kg body weight) via subcutaneous osmotic minipumps. OA-NO_2 significantly inhibited atrial fibrosis and depressed vulnerability for AF during right atrial electrophysiological stimulation to levels observed for AngII-naive animals. Left atrial epicardial mapping studies demonstrated preservation of conduction homogeneity by OA-NO_2. The protection from fibrotic remodelling was mediated by suppression of Smad2-dependent myofibroblast transdifferentiation and inhibition of Nox2-dependent atrial superoxide formation.

Conclusion OA-NO_2 potently inhibits atrial fibrosis and subsequent AF. Nitro-fatty acids and possibly other lipid electrophiles thus emerge as potential therapeutic agents for AF, either by increasing endogenous levels through dietary modulation or by administration as synthetic drugs.

Keywords Atrial fibrillation • Fibrosis • Nitro-fatty acids • Reactive oxygen species

1. Introduction

Atrial fibrillation (AF) represents the most common rhythm disorder with a life-time risk for those reaching 40 years of age of 25% in Europe and the USA.[1] This arrhythmia is associated with a 2-fold increase in risk for death, due to a substantially increased risk for stroke.[1] Atrial fibrosis contributes to the pathogenesis of AF, as it interferes with electrical conduction by disrupting cardiomyocyte coupling.[2] Atrial fibrotic remodelling is a consequence of impaired extracellular matrix (ECM) turnover due to excessive deposition of collagen. Myofibroblast differentiation from cardiac fibroblasts, a consequence of the pro-fibrotic and pro-inflammatory reactions induced by transforming growth factor-β (TGF-β) and angiotensin II (AngII), leads to collagen accumulation, elevated rates of production of reactive oxygen species, and left atrial remodelling.[3]

Nitro-fatty acids (NO_2-FA) are electrophilic signalling mediators, which are generated by the reaction of nitrogen dioxide with unsaturated fatty acids, a reaction orders of magnitude more facile than nitration of tyrosine.[4] NO_2-FA are detected in species ranging from plants to humans and are generated by nitrogen dioxide arising from both oxidative inflammatory and metabolic reactions dependent on nitric oxide and nitrite. NO_2-FA and other 'soft' lipid electrophiles reversibly react

* Corresponding author. Tel: +49 221 478 32495; fax: +49 221 478 32496, E-mail: volker.rudolph@uk.koeln.de

† These authors contributed equally to the manuscript.

via Michael addition with nucleophilic residues such as the hyperreactive cysteines of proteins.[5] NO_2-FA mediate anti-inflammatory signalling actions via the modulation of signalling pathways including nuclear factor erythroid 2-related factor 2/kelch-like ECH-associated protein 1 (Nrf2/Keap-1)-regulated heme oxygenase 1 (HO-1) expression, nuclear factor kappa light chain enhancer of activated B cells (NF-κB) and mitogen-activated protein kinase (MAP kinase).[6] Recent studies have shown that dietary interventions can increase endogenous levels of these compounds,[7] and USFDA-approved Phase 1 safety and efficacy studies for synthetic NO_2-FA are underway.

Given the prominent role of inflammation in the pathogenesis of AF and atrial fibrosis, we evaluated whether an exemplary NO_2-FA, nitro-oleic acid (OA-NO_2), suppresses development of atrial fibrosis and vulnerability to AF in a murine model of AngII-induced AF.

2. Methods

2.1 Animal model and handling

Wild-type C57BL/6J mice were treated for 2 weeks with AngII (1.5 ng/g/min, Sigma-Aldrich, St Louis, USA) and nitro-oleic acid (6 mg/kg) solvated in polyethylene glycol/ethanol (90 : 10, vol/vol) or vehicle (polyethylene glycol/ethanol, 90 : 10), via subcutaneous implantation of osmotic minipumps (ALZET, Cupertino, CA, USA). Nitro-oleic acid (OA-NO_2) was provided from the lab of Bruce Freeman, PhD, University of Pittsburgh.

Animal groups:

Mice without AngII and OA-NO_2	−AngII(−)/OA-NO_2(−) group
Mice with AngII and without OA-NO_2	−AngII(+)/OA-NO_2(−) group
Mice with AngII and with OA-NO_2	−AngII(+)/OA-NO_2(+) group

All animal procedures were performed with isofloran anaesthesia and analgesia with buprenorphine. Euthanasia was performed by heart excision in deep anaesthesia. All animal studies were approved by the local authorities (Behörde für Soziales, Familie, Gesundheit und Verbraucherschutz, Fachabteilung Veterinärwesen und Lebensmittelsicherheit, Hamburg,G09/064 and Landesamt für Natur, Umwelt und Verbraucherschutz Nordrhein-Westfalen, 84-02.04.2012.A307) and by the Universities of Hamburg and Cologne Animal Care and Use Committees. Animal experiments conform to the guidelines from Directive 2010/63/EU of the European Parliament on the protection of animals used for scientific purposes. Observers were blinded for all quantitative analyses.

2.2 Electrophysiological investigation

Invasive right atrial stimulation was performed as described previously.[8] In brief, an octapolar electrophysiological catheter (1.1 F, Scisense, London, Canada) was inserted via the right jugular vein to the right atrium and ventricle. Intracardiac atrial and ventricular recording and atrial stimulation manoeuvres were performed using a CardioTek EPTracer (Biotronik, Berlin, Germany). Bipolar electrograms were obtained from each electrode pair during the whole procedure. Programmed atrial stimulation was performed at pacing stimulus amplitudes of 1.0 and 2.0 mA with 7 stimuli fixed rate at S1S1 cycle length of 120, 110, and 100 ms, respectively, with one short coupled extra stimulus with a 10 ms stepwise S1S2 reduction starting at cycle length of 80 ms down to 10 ms. Atrial burst stimulation was performed for 1 s (three times consecutively) at S1S1 stimulation cycle lengths starting at 50 ms with 10 ms stepwise reduction down to 10 ms at pacing stimulus amplitudes of 1.0 and 2.0 mA. Between these stimulation procedures, a 10 s recovery period was maintained. AF was defined by the presence of rapid and fragmented atrial electrograms in combination with irregular AV-nodal conduction and ventricular rhythm with a duration of these atrial electrograms of >1 s. The number of AF episodes and AF duration (last stimulus-spike to the first sinus-rhythm P wave) was analysed.

2.3 *Ex vivo* electrophysiological atrial mapping

For atrial electrophysiological mapping, hearts of mice were excorporated and cannulized with a blunted canula, connected to a Langendorff system, and retrogradely perfused via the aorta and the coronary arteries with a carbogen gas flushed Krebs Henseleit buffer with a constant flow of 1.5 mL/min. A 32-electrode microelectrode array (MEA, Multichannel Systems, Reutlingen, Germany) was positioned on the epicardial surface of the right atrium. Electrograms were recorded using a 128-channel, computer-assisted recording system (Multichannel Systems) with a sampling rate of 25 kHz (25 000 samples/s). Data were bandpass filtered (50 Hz), digitized with 12 bits and a signal range of 20 mV. Activation maps were calculated from these data using custom-programmed software (Excel, Microsoft, Redmond, WA, USA). The first derivative of each unipolar electrogram was evaluated, and the minimum of d*V*/d*t* activation was defined as time point of local activation for pacing studies. To obtain an index of local conduction slowing for each electrode, the activation time differences to neighbouring points were normalized to inter-electrode distance (300 μm). The largest difference at each site is defined as local phase delay. The average phase delay and the absolute inhomogeneity of phase delays were calculated and used as index for smoothness in global conduction. For pacing studies, the hearts were stimulated with a concentric bipolar electrode (FHC, Bowdoin, USA) with a stimuli rate of 7 Hz at the aortic root.

2.4 Patch clamp technique

Action potential (AP) measurements of ventricular cardiomyocytes were performed as previously described. [Schwoerer Ehmke, JMCC 2008; PMID:18721926] Left ventricular cardiac myocytes were enzymatically isolated from 8- to −12-week-old male FVB/N mice. APs were measured using the patch-clamp technique. Extracellular solution consisted of a modified Tyrodes solution containing (in mmol/L): NaCl 138, KCl 4, $MgCl_2$ 1, NaH_2PO_4 0.33, $CaCl_2$ 2, Glucose 10, HEPES 10, titrated to pH = 7.30 with NaOH. Pipette solution contained (mmol/L): K-glutamate 120, KCl 10, $MgCl_2$ 2, EGTA 10, HEPES 10, Na_2-ATP 2, titrated to pH = 7.20 with KOH. For AP measurements, the cells were stimulated at room temperature at a frequency of 1 Hz using 5−10 ms short depolarizations at 150% of the AP threshold. APs were assessed under control conditions for 1 min in the modified Tyrode solution and following wash-in of 0.1% ethanol (solvent for OA-NO_2) for a period of 5 min. Finally, APs were measured for 5 min when the cells were incubated with 5 μmol/L OA-NO_2. Experiments were performed and analysed using the Pulse software (HEKA Electronic, Lambrecht, Germany) and Igor (WaveMetrics, Lake Oswego, OR, USA).

2.5 Masson's trichrome and Picrosirius red staining of atrial sections

Amount of atrial fibrosis was determined by performing both Picrosirius red and Masson's trichrome staining. Paraffin-fixed atrial sections were stained with either Picrosirius red or Goldner Solutions I−III (Carl Roth GmbH, Germany), respectively. Planimetry was performed with IVision software (BioVision Technologies, Exton, PA, USA).

2.6 Cell culture

The murine RAW 264.7 macrophages and NIH/3T3 fibroblasts (ATCC, Manassas, VA, USA) were seeded to 6-well plates and left to adhere in DMEM (PAN-Biotech, Aidenbach, Germany) supplemented with 10% of fetal bovine serum (FBS, low endotoxin; PAA, Pasching, Austria) and 1% gentamycin. Immediately before the start of experiments, the complete DMEM medium was replaced by FBS-free DMEM, and cells were cultivated with OA-NO_2 (0.1−1 μM) for harvest at different time points, as indicated in Results section.

2.7 RAW 264.7 macrophage and fibroblast ROS generation

Chemiluminescence (CL) was measured using a microplate luminometer LM-01T (Immunotech, Prague, Czech Republic). Briefly, macrophages cultivated in FBS-free DMEM medium were activated with phorbol-12-myristate-13-acetate (PMA) at 97.6 μg/mL in the presence of 1 mM luminol. The CL emission representing the oxidative burst was monitored for 4 h at 37°C, and the integral value of the CL reaction was recorded. Recognizing that luminol chemiluminescence has limitations in the measurement of reactive species, an alternative strategy was also used for detection of rates of reactive oxygen species (ROS) production by macrophages.[9] The extracellular production of superoxide anion by RAW 264.7 macrophages and 3T3 fibroblasts was determined using spectrophotometric analysis of cytochrome c reduction (final concentration 100 μM). The reduction of cytochrome c was monitored at 550 nm, and the difference in absorbance between individual time points was converted to equivalent O_2^- production using the molar extinction coefficient for cytochrome c (21.1 mM^{-1} cm^{-1}).

2.8 IF of α-smooth muscle actin and connexin 43

Hearts were frozen in OCT compound and cut to 4 μm longitudinal sections. Sections were thawed, were fixed with 3.7% formaldehyde solution, and were blocked with 10% mouse serum. Slides were treated with 0.1% Triton X-100 and incubated either with primary antibody against α-smooth muscle actin (α-SMA; 1 : 200, rabbit IgG, ab5694, Abcam, Cambridge, UK) and DDR-2 (1 : 50, goat IgG, sc7555, Santa Cruz, TX, USA) or with primary antibody against connexin 43 (Cx43; 1 : 1000, rabbit IgG, C6219-2 ML, Sigma-Aldrich, USA) and N-cadherin (1 : 1000, rabbit IgG, sc-1502, Santa Cruz, USA) for 1 h at RT in PBS with 0.1% Triton-X100 and 10% mouse serum. Secondary antibody was Alexa Fluor-594 chicken anti-rabbit IgG and Alexa Fluor-488 chicken anti-goat IgG (Invitrogen) and nuclei were stained with DAPI. Images were taken with a Retiga 1300 CCD camera mounted on Leica DMLB fluorescence microscope by iVision v4.0. For imunostaining of NIH/3T3 fibroblasts, BD Falcon CultureSlides were used. Cells were fixed with 4% formaldehyde, permeabilized using 0.1% Triton X-100, and blocked with 10% goat serum. Primary antibody against α-SMA (1 : 100, mouse IgG; Biomeda V1031), goat anti-mouse IgG (H + L) secondary antibody, DyLight 488 conjugate (Thermo Scientific) were used. Nuclei were stained with DAPI. Images were taken with a Retiga 1300 CCD camera mounted on Leica DMLB fluorescence microscope by iVision v4.0. Quantification of myofibroblasts was performed by counting α-SMA/DDR2-positive cells in atrial sections. The observer was blinded during the quantification.

2.9 Dihydroethidium staining of atrial sections

Frozen atrial sections were stained with dihydroethidium (DHE, 5 μM, diluted in DMSO and HBSS buffer) as another index of oxidant generation.[10] The slides were incubated with DHE for 30 min at 37°C in the dark before pictures were taken with a fluorescence microscope (DMLB, Leica, Solms, Germany) and planimetrically quantificated by using IVision software (BioVision Technologies, Exton, PA, USA).

2.10 Detection of protein expression by western blot analysis

Equal amounts of protein (20 μg) from each cell lysate were subjected to SDS–PAGE. The protein was then transferred to polyvinylidene difluoride (PVDF) membranes (Immobilon-P, Millipore, Billerica, MA, USA) and incubated with antibodies against α-smooth muscle actin (Santa Cruz Biotechnology, Santa Cruz, CA, USA), p38 MAPK, phospho-p38 MAPK (Thr180/Tyr182), Smad2, and phospho-Smad2 (Ser 465/467) (all purchased from Cell Signaling Technology, Danvers, MA, USA). Membranes were further incubated with secondary antibodies conjugated with horseradish peroxidase. The blots were visualized using SuperSignal West Pico Chemiluminescent Substrate (Pierce, Rockford, IL, USA) and exposed to CP-B X-ray films (Agfa, Brno, Czech Republic). The relative levels of proteins were quantified by scanning densitometry using the ImageJ™ program (National Institutes of Health, Bethesda, MD, USA), with the individual band density value expressed in arbitrary units (optical density, OD). Equal protein loading was verified by β-actin or α-tubulin immunoblotting (Santa Cruz Biotechnology).

2.11 Statistical analysis

One-way ANOVA test, followed by Fisher's least significant difference (LSD) *post hoc* test was used for comparison of treatment groups. Alternatively, Student's *t*-test was used as appropriate for comparisons between treatment groups. In the figures, statistical significance is mentioned with the asterisks *, **, and *** standing for a *P*-value of 0.05, 0.01, and 0.001, respectively. Results are expressed as mean values ± SEM. Data were analysed with SPSS statistical software (IBM, Cologne, Germany) or Prism (Graphpad, La Jolla, CA).

3. Results

3.1 OA-NO_2 reduces the vulnerability for AF in AngII-treated mice

After 2 weeks of continuous AngII administration, the number of AF episodes as well as the total time of episodes upon electrophysiological stimulation was markedly increased in AngII(+)/OA-NO_2(−) mice compared with AngII(−)/OA-NO_2(−) mice (*Figure 1A–C*). Treatment with OA-NO_2 reduced AF vulnerability in AngII(+)/OA-NO_2(+) mice with reductions in both number and total time of AF episodes to the level of AngII-naive animals (*Figure 1B* and *C*). To control for direct interference of OA-NO_2 with Ang II release from the osmotic minipumps, Ang II plasma levels were measured after 2 weeks. AngII plasma levels were significantly higher in both AngII(+)/OA-NO_2(−) and AngII(+)/OA-NO_2(+) mice compared with AngII (−) animals, whereas no significant difference was observed between AngII(+)/OA-NO_2(−) and AngII(+)/OA-NO_2(+) mice (see Supplementary material online, *Figure S1*).

3.2 OA-NO_2 suppresses atrial fibrosis and preserves atrial conduction homogeneity

Fibrosis is an established substrate of AF. A trichrome staining of paraffin-embedded murine atrial sections revealed significantly greater atrial fibrosis in AngII(+)/OA-NO_2(−) mice compared with AngII(−)/OA-NO_2(−) animals (*Figure 2A*). Compared with AngII(+)/OA-NO_2(−) mice, AngII(+)/OA-NO_2(+) mice exhibited significantly reduced levels of atrial fibrosis, which were in fact equivalent to those of AngII-naive animals (*Figure 2B*). These findings corresponded to changes in conduction properties assessed by epicardial mapping (*Figure 2C*). Thus, absolute inhomogeneity and mean latency were significantly increased in AngII(+)/OA-NO_2(−) mice compared with AngII(−)/OA-NO_2(−) animals, whereas this effect of Ang II was completely abolished in AngII(+)/OA-NO_2(+) mice (*Figure 2D* and *E*). Of note, absolute inhomogeneity showed a significant correlation with the amount of collagen deposition determined by trichrome staining (Pearson's *r*: 0.643, $P = 0.01$). Furthermore, a Picrosirius red staining of another cohort of animals confirmed the results of the trichrome staining (*Figure 2F* and *G*).

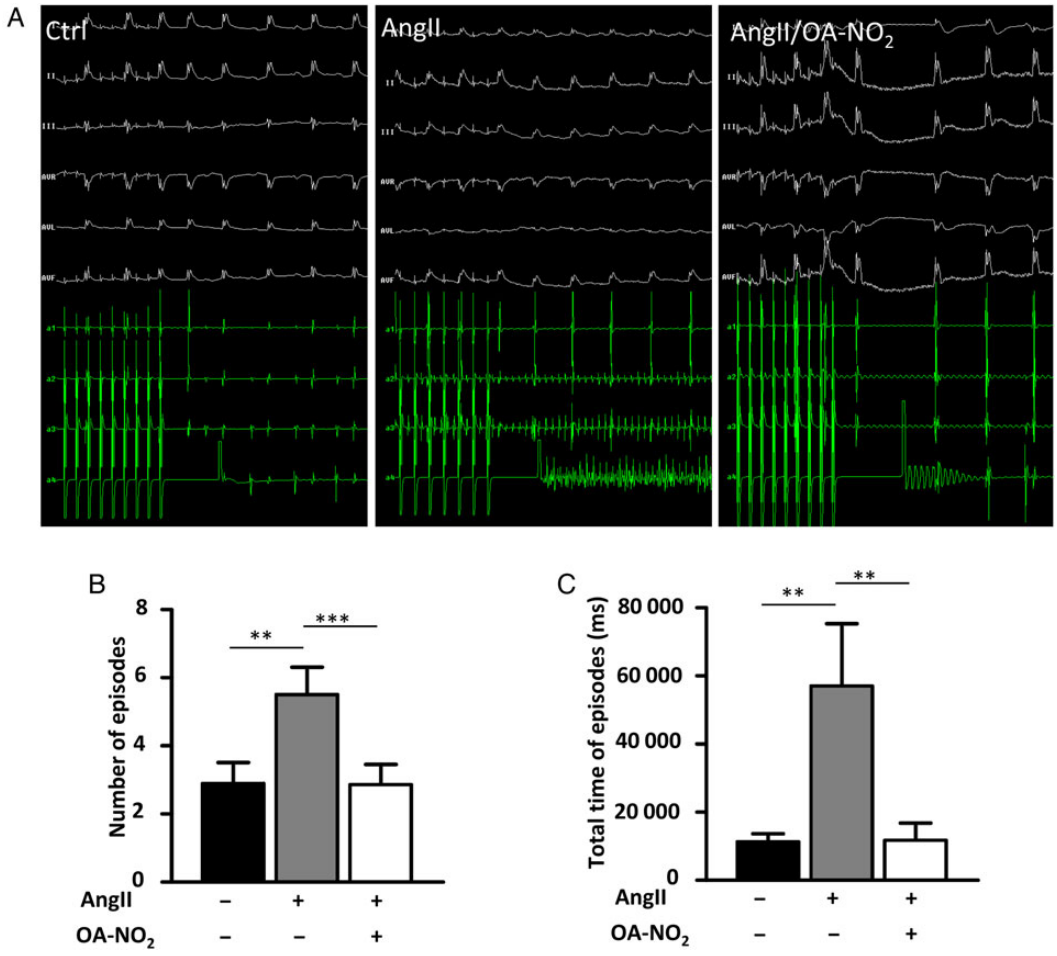

Figure 1 OA-NO_2 treatment attenuates elevated vulnerability for atrial fibrillation and restores electrical homogeneity in AngII-treated mice. AngII and OA-NO_2 were administered over a period of 2 weeks via osmotic minipumps (Alzet), and afterwards, the mice underwent an electrophysiological study with right atrial stimulation. (*A*) Representative figures of ECGs with and without fibrillation episodes. (*B*) AngII treatment leads to a distinct elevation of the number of AF episodes in AngII(+)/OA-NO_2(−) mice ($n = 14$), whereas notably in AngII(+)/OA-NO_2(+) mice ($n = 7$), the number of AF episodes is comparable to the control group [AngII(−)/OA-NO_2(−) mice] ($n = 19$). (*C*) The total time of AF episodes was calculated and the prolonged time of AF episodes was significantly reduced in AngII(+)/OA-NO_2(+) ($n = 7$) compared with AngII(+)/OA-NO_2(−) mice ($n = 14$). Data are expressed as mean ± SEM. $^{**}P < 0.01$ and $^{***}P < 0.001$.

3.3 Effect of OA-NO_2 on cardiomyocyte AP and Cx43

Assessment of key parameters of cellular electrophysiology (resting membrane potential, AP overshoot, and duration) of left ventricular cardiomyocytes was unaffected by OA-NO_2 (see Supplementary material online, *Figure S2A–C*). Also no effect of OA-NO_2 on the expression and distribution of Cx43, which has been shown to critically contribute to cardiomyocyte coupling in the context of AF, could be observed (see Supplementary material online, *Figure S2D* and *E*).[11–13]

3.4 OA-NO_2 inhibits fibroblast transdifferentiation to myofibroblasts by inhibition of Smad2 activation

Co-staining of atrial tissue with DDR2 (tyrosine kinase receptor for fibrillar collagen) and α-SMA (marker of myofibroblasts) revealed a significant increase in myofibroblasts in AngII(+)/OA-NO_2(−) compared with AngII(−)/OA-NO_2(−) animals. In AngII(+)/OA-NO_2(+), this effect was almost completely blunted (*Figure 3A* and *B*). In accordance, TGF-β-induced differentiation of 3T3 fibroblasts to myofibroblasts was significantly reduced by incubation of the cells with 1 μM OA-NO_2 as indicated by α-SMA expression in western blot analysis and immunofluorescent staining (*Figure 3C* and *D*). These findings were corroborated by α-SMA expression analysis of isolated murine cardiac fibroblasts, which revealed a significant OA-NO_2-dependent reduction of α-SMA expression in these cells (see Supplementary material online, *Figure S3*). Moreover, TGF-β induced activation of Smad2 in 3T3 fibroblasts was significantly attenuated by OA-NO_2 (1 μM), as indicated by western blot analysis of Smad2 phosphorylation (Ser 465/467, *Figure 3E*).

3.5 OA-NO_2 reduces atrial oxidative inflammatory mediator generation

To further substantiate the observed effects of OA-NO_2, we investigated its effect on atrial oxidant formation as a contributing factor to

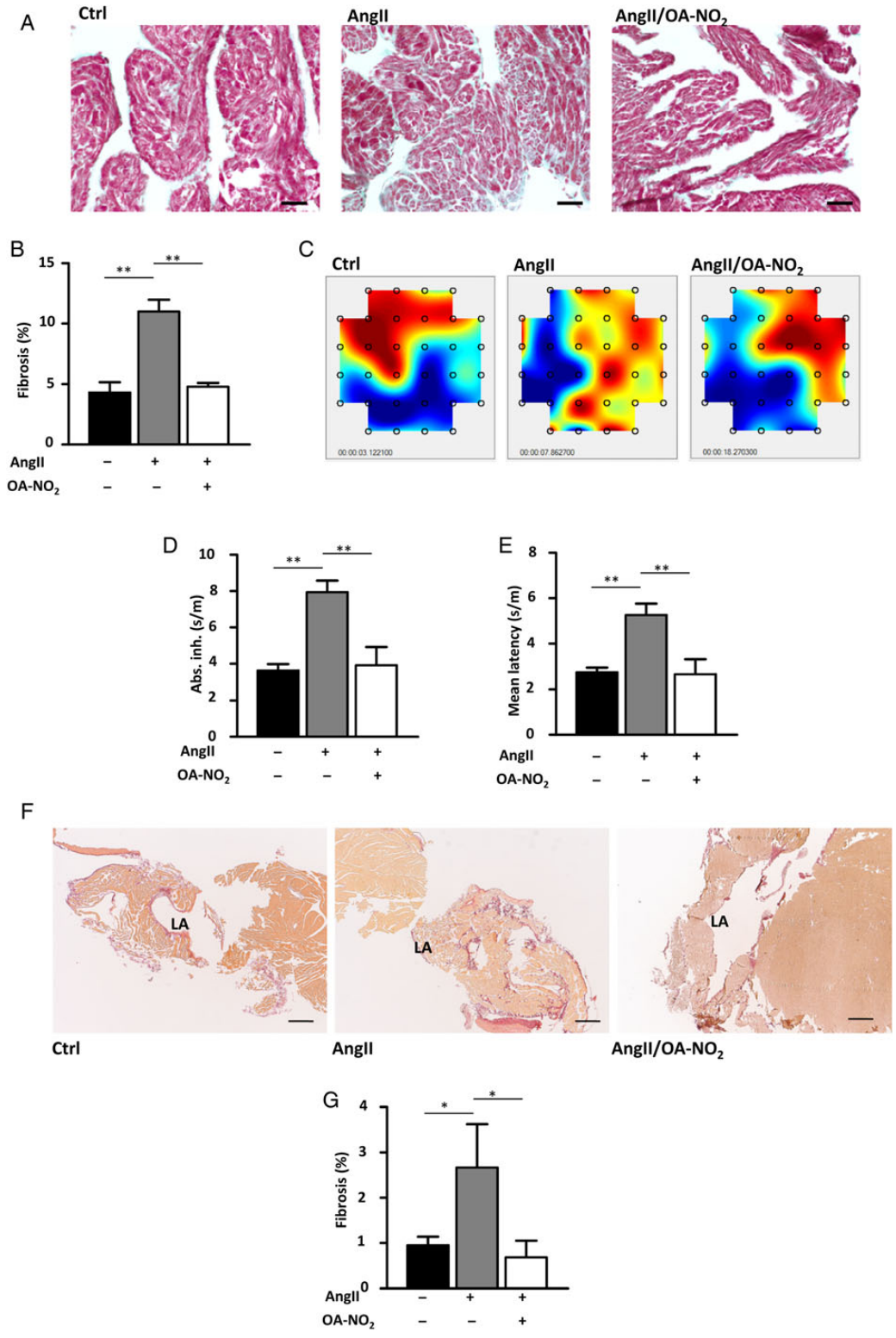

Figure 2 Electrical conductance and atrial fibrosis. OA-NO_2 reduces extents of atrial fibrosis in AngII-treated mice. Paraffin-embedded atrial sections were subjected to Masson's trichrome staining. (*A*) Representative images of trichrome-stained atrial sections. Scale bar indicates 750 μm. (*B*) Quantification of fibrotic areas AngII(+)/OA-NO_2(−) ($n = 5$) animals show an higher extent of atrial fibrosis, while concomitant OA-NO_2 treatment leads to a significant reduction of atrial fibrotic areas AngII(+)/OA-NO_2(+)-treated animals ($n = 6$). (*C*) Representative images of epicardial mappings performed with the same hearts subjected to the trichrome staining. (*D* and *E*) Measurement of absolute inhomogeneity and mean latency by epicardial mapping closely reflected changes observed in atrial fibrosis ($n = 5, 6, 5$), with a significant correlation between absolute inhomogeneity and the amount of atrial fibrosis. (*F*) Representative images of Picrosirius red-stained atrial sections. Scale bar indicates 1500 μm. (*G*) Quantification of the Picrosirius red staining corroborates the results of the trichrome staining ($n = 9, 8, 7$). Data are expressed as mean ± SEM. $^*P < 0.05$ and $^{**}P < 0.01$.

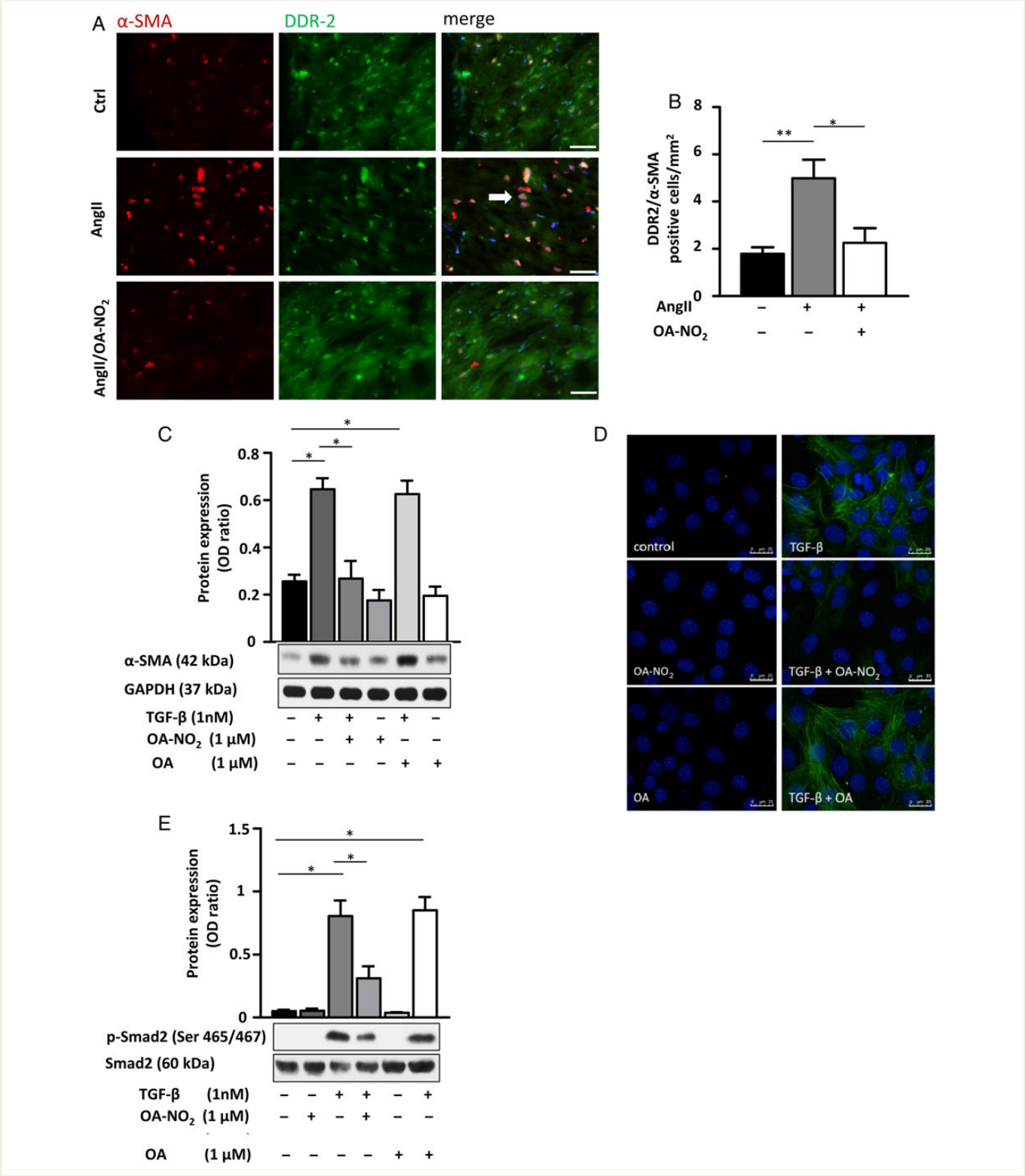

Figure 3 $OA\text{-}NO_2$ inhibits fibroblast differentiation by inhibition of Smad-2 activation. (*A* and *B*) DDR2/α-SMA co-staining of murine atrial sections shows a significant higher amount of myofibroblasts in atrial tissue of AngII(+)/$OA\text{-}NO_2$(−) mice ($n = 5$) compared with the control group [AngII(−)/$OA\text{-}NO_2$(−)] ($n = 5$), while $OA\text{-}NO_2$ treatment ($n = 4$) reduced the number of myofibroblasts to the level of control animals. Representative arrow indicates co-localization of DDR2 and α-SMA. Scale bar indicates 40 μm. (*C* and *D*) Treatment of 3T3 fibroblasts with TGF-β (5 ng/mL) and/or $OA\text{-}NO_2$ (1 μM) for 8 h reveals an inhibition of TGF-β-induced fibroblast differentiation by $OA\text{-}NO_2$ evidenced by western blot analysis and immunofluorescent staining. Pooled data from four independent experiments are shown. Scale bar indicates 25 μm. (*E*) $OA\text{-}NO_2$ reduces TGF-β-induced phosphorylation of Smad-2 (Ser 465/467) in 3T3 fibroblasts, as detected by western blot. Pooled data from three independent experiments are shown. Data are expressed as mean ± SEM. $^*P < 0.05$ and $^{**}P < 0.01$.

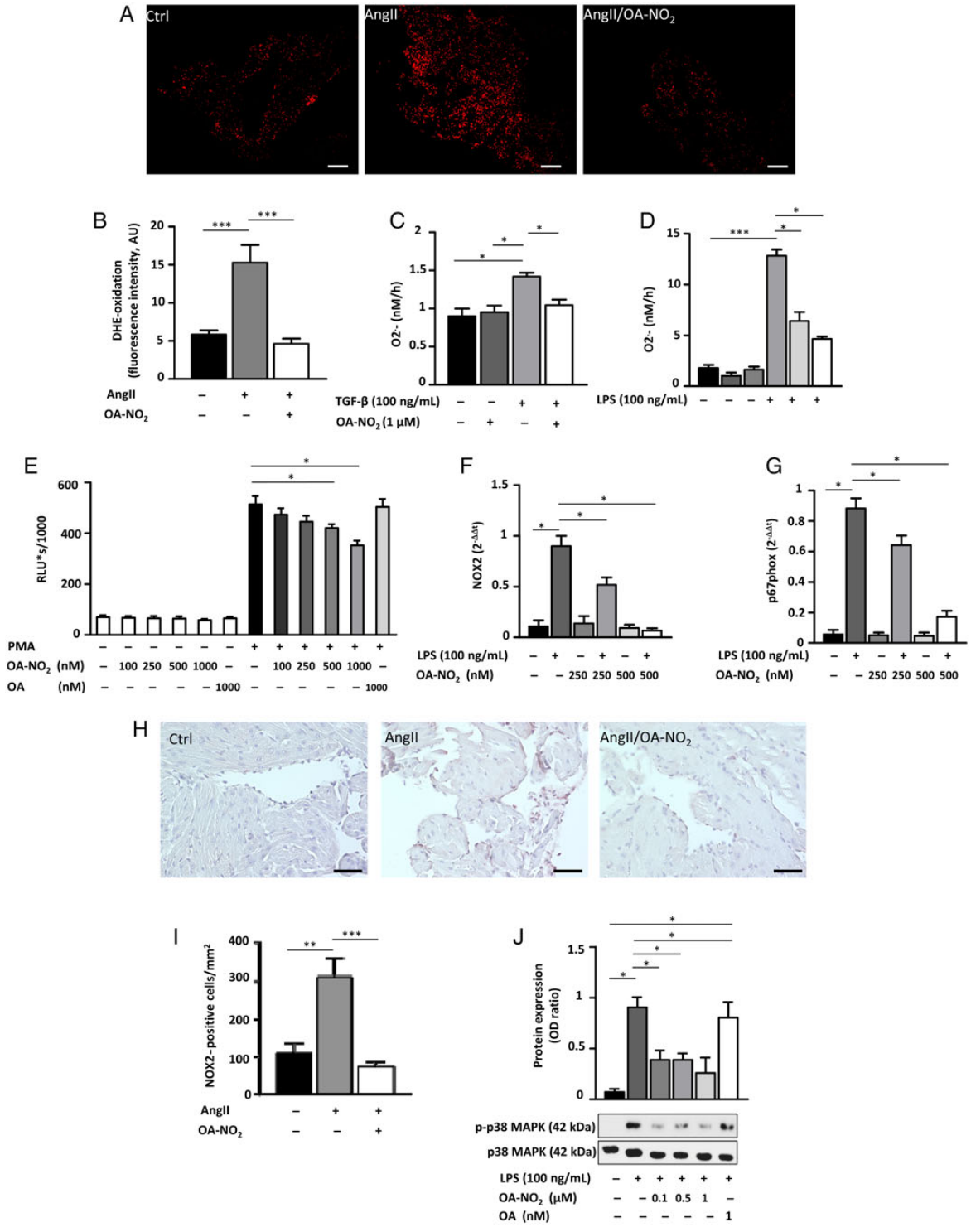

Figure 4 $OA\text{-}NO_2$ inhibits atrial generation of reactive inflammatory mediators. (*A* and *B*) DHE stainings of atrial sections reveal a significantly reduced ROS formation in AngII(+)/$OA\text{-}NO_2$(+) mice ($n = 8$) compared with AngII(+)/$OA\text{-}NO_2$(−) animals ($n = 7$), with ROS levels in AngII(+)/$OA\text{-}NO_2$(+) equalling those of control animals ($n = 8$). Scale bar indicates 750 μm. (*C*) TGF-β-induced superoxide production measured by cytochrome c reduction assay in 3T3 fibroblasts is significantly blunted upon $OA\text{-}NO_2$ treatment ($n = 5$). (*D*) LPS-induced production of superoxide in murine peritoneal RAW 264.7 macrophages measured by cytochrome c reduction assay is inhibited by $OA\text{-}NO_2$ in a dose-dependent manner ($n = 6$). (*E*) Oxidative burst in murine peritoneal RAW 264.7 macrophages induced by phorbol-12-myristate-13-acetate (PMA) is also reduced by application of $OA\text{-}NO_2$ ($n = 4$). (*F* and *G*) The LPS-induced expression of NOX2 as well as of its cytosolic regulatory protein p67phox is significantly attenuated by $OA\text{-}NO_2$ treatment in a dose-dependent manner ($n = 5$). (*H* and *I*) NOX2 stainings of atrial sections reveal a significantly reduced NOX2 expression in AngII(+)/$OA\text{-}NO_2$(+) mice ($n = 8$) compared with AngII(+)/$OA\text{-}NO_2$(−) animals ($n = 7$), with ROS levels in AngII(+)/$OA\text{-}NO_2$(+) equalling those of control animals ($n = 8$). Scale bar indicates 50 μm. (*J*) $OA\text{-}NO_2$ decreases phosphorylation of p38 MAPK. Pooled data from four independent experiments are shown. Data are expressed as mean ± SEM. $^*P < 0.05$, $^{**}P < 0.01$, and $^{***}P < 0.001$.

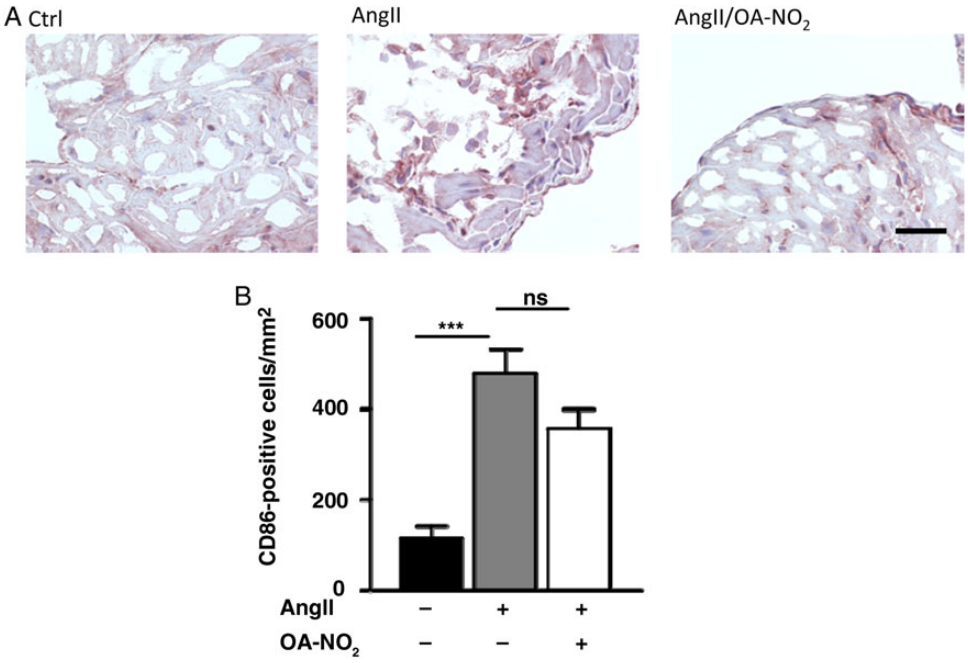

Figure 5 Number of CD86-positive cells in atrial tissue. (*A*) Representative figures of an immunohistological staining of atrial sections by using an anti-CD86-specific antibody. (*B*) Quantification of CD86-positive cells in atrial tissue reveal a significant higher amount of these cells in AngII (+)/OA-NO_2 (−) animals ($n = 5/4/4$). Furthermore, this was not significantly influenced by a parallel treatment with OA-NO_2. For the staining of paraffin-embedded murine atrial sections with CD86 (1 : 500, rabbit IgG, NB110−55488, Novus Biologicals, USA), a standard protocol was used. For quantification, CD86-positive cells were counted in atrial sections. Scale bar = 50 μm. ***$P < 0.001$.

atrial fibrotic remodelling and arrhythmogenicity. There was a significant reduction in DHE oxidation by atrial tissues in AngII(+)/OA-NO_2(+) animals compared with AngII(+)/OA-NO_2(−) animals, which tended to be suppressed even more than in AngII-naive animals (*Figure 4A* and *B*). In accordance, there was an OA-NO_2-mediated decrease in superoxide production by fibroblasts and macrophages (*Figure 4C–E*). Using murine peritoneal RAW 264.7 macrophages, there was a dose-dependent reduction of both NOX2 and its cytosolic regulatory protein p67phox expression as a key mechanism accounting for decreased ROS production by OA-NO_2 (*Figure 4F* and *G*). In addition, NOX2 staining of paraffin-embedded atrial sections revealed a significant higher amount of NOX2-positive cells in AngII(+)/OA-NO_2(−) animals, which was significantly reduced following OA-NO_2 administration (*Figure 4H* and *I*). Western blot analyses furthermore revealed a decreased phosphorylation of p38 MAP kinase. (*Figure 4J*). Of interest, a significantly higher amount of M1 polarized macrophages in atria of AngII(+)/OA-NO_2(−) animals assessed by a CD86 immunohistology was not influenced by an additional OA-NO_2 treatment (*Figure 5A* and *B*).

4. Discussion

Herein it is shown that *in vivo* NO_2-FA administration potently reduced atrial fibrotic remodelling as well as susceptibility to AF and conduction inhomogeneity in AngII-pretreated mice. These anti-fibrotic effects of NO_2-FA were mediated by Smad2-related suppression of myofibroblast differentiation, as well as inhibition of atrial generation of oxidative inflammatory mediators (*Figure 6*).

Atrial fibrosis is a significant pathophysiological factor, which has been postulated to underlie most forms of AF.[2] It has been documented in patients with structural heart disease[14] and patients with lone AF,[15] correlating with AF persistence.[16] Mechanistically, atrial fibrosis disrupts cell−cell coupling between cardiomyocytes, thereby not only provoking inhomogeneities of electrical conduction (which favour re-entrant circuits[17]) but also facilitating ectopic activity due to early and delayed after-depolarizations.[18]

AngII is a central signalling mediator in the pathogenesis of atrial fibrosis, with AngII expression increased in patients with AF.[19] Moreover, rapid atrial pacing leads to secretion of AngII[20] and cardiac overexpression of angiotensin-converting enzyme leads to atrial fibrosis and AF.[21] In our AngII-dependent murine model of AF, OA-NO_2 completely abolished the pro-fibrotic effects of AngII treatment. Importantly, this inhibitory effect of OA-NO_2 on fibrotic remodelling is confirmed by two different quantitative stainings of atrial fibrosis derived from two independent sets of animals. Moreover, the relevance of atrial fibrosis on the observed susceptibility for AF is not only strongly supported by epicardial contact mapping studies showing complete reversal of the AngII-induced increase in latency and inhomogeneity of conduction by OA-NO_2 but also by the significant correlation observed between extent of atrial fibrosis assessed by trichrome staining and absolute inhomogeneity assessed by epicardial mappings performed in the same hearts.

Mechanistically, myofibroblasts are a hallmark of pathological fibrotic remodelling of the myocardium. Their differentiation from fibroblasts, which is induced by haemodynamic, neurohumoral, and inflammatory mediators, is essential for stimulating extracellular collagen deposition and the increased arrhythmogenicity observed in this context.[22] There

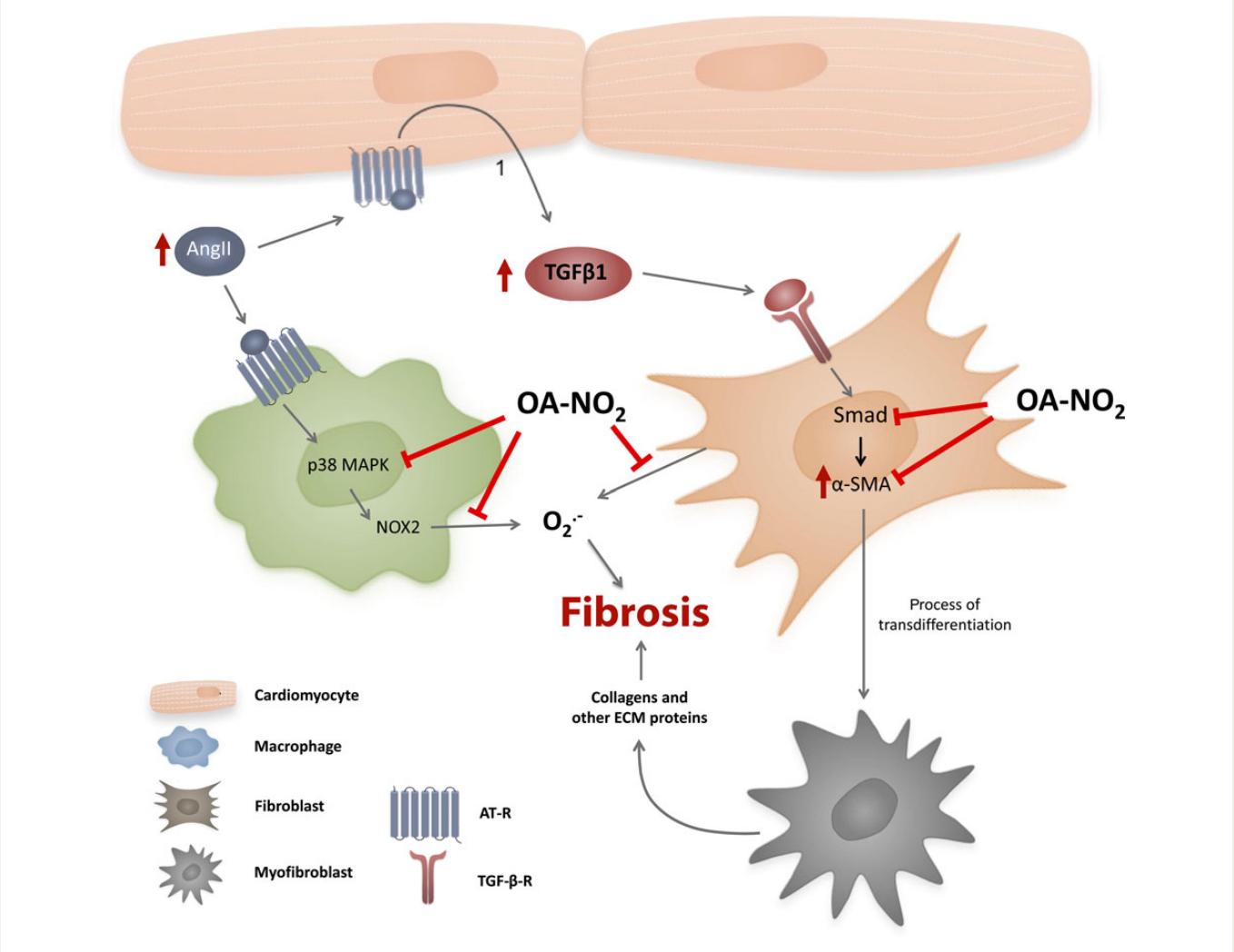

Figure 6 Proposed mechanism by which OA-NO_2 reduces fibrosis in the atrium of AngII-treated mice. OA-NO_2 decreases fibroblast transdifferentiation through inhibition of Smad-2 activation, as indicated by a reduction of α-SMA expression. Additionally, OA-NO_2 reduces atrial oxidative stress due to attenuation of superoxide production from macrophages and fibroblasts by inhibition of NOX2 and p67 phox expression via p38 MAPK deactivation.

was a significant inhibition of both AngII-mediated myofibroblast formation and TGF-β-induced, Smad 2-dependent fibroblast differentiation by OA-NO_2. In addition to being a key source of collagen during fibrotic remodelling, myofibroblasts also exert potent autocrine and paracrine actions, including secretion of TGF-β and even AngII and thus perpetuate a vicious circle leading to progressive atrial fibrosis.[22] The importance of interrupting this vicious circle by abrogating the formation of this cell type, as by OA-NO_2-induced signalling responses, can thus not be overstated.

Patient tissue studies reveal an association between oxidative protein modifications and AF.[23] These studies are flanked by more mechanistic studies in transgenic mice, pigs, and human tissue, which reveal a crucial role for oxidative inflammatory mediators in the pathobiology of AF.[3] In particular, a study using cardiac-specific Rac1-overexpression, a regulator of NADPH oxidase, showed increased atrial fibrosis due to NADPH oxidase-dependent superoxide production and reactions.[24] The present data reveal a markedly decreased formation of this and related reactive species in atrial tissue upon treatment with OA-NO_2 (*Figure 4B*). This finding is mirrored by a pronounced suppression of superoxide production by fibroblasts and macrophages. These two cell types are important sources of superoxide in AF, as fibroblasts are the most abundant cells in the heart and macrophages, which are recruited to atrial tissue as a consequence of AF,[25] are among the most highly active tissue sources of superoxide production.[26] The impact of OA-NO_2 on inhibiting oxidant generation formation is reinforced by the decreased expression of NOX2 assessed in atrial tissue and isolated macrophages, the NOX2 subunit p67phox, and the inhibition of p38 MAP kinase phosphorylation, a critical regulatory step in both NOX2 expression and its activation by phosphorylation.[27] Notably, NOX2 is a major superoxide and downstream oxidant source in multiple cell types, including macrophages and fibroblasts.[28] Importantly, previous studies have demonstrated that superoxide produced by activated macrophages is almost exclusively formed by NOX2, supporting[29] the fact that OA-NO_2 not only suppresses expression but also activity of NOX2.[30]

This study used a murine model of AF induction by right atrial stimulation. Thus, a number of limitations may apply when trying to translate the present findings to human pathology. The mechanisms underlying AF in humans are complex and to date remain incompletely understood. Multiple theories have evolved from findings stemming from

electrophysiological mapping studies, including the multiple wavelet and leading circle concept, but also more recent models suggesting spiral waves or rapidly firing ectopic foci evoked by early and delayed after-depolarizations. The mouse model used herein is not suitable to investigate these mechanisms. However, the main focus of this study was to assess the effect of OA-NO_2 on atrial fibrosis as a crucial substrate for most of the above-noted models of AF, for which murine models have been widely used.[21] The increased inducibility of AF demonstrated in this work underpins the relevance of the observed effects of OA-NO_2 on suppressing atrial fibrosis. Furthermore, it has to be noted that OA-NO_2 also inhibits angiotensin 1 receptor activation,[31] thus it cannot be ruled out that the observed *in vivo* effects of OA-NO_2 on AF and atrial fibrosis observed herein are partially related to inhibition of the angiotensin 1 receptor activation. However, our *in vitro* data showing OA-NO_2-mediated reduction in TGF-β-induced myofibroblast transdifferentiation and inhibition of macrophage superoxide production reveal effects of OA-NO_2 beyond direct inhibition of AngII 1 receptor activation. These considerations are relevant, as they suggest a broader applicability of these results, which are not merely restricted to the AF model employed herein. They are also of relevance considering the fact that AngII inhibition in patients with AF yielded variable results.[32]

In conclusion, the nitro-fatty acid OA-NO_2 potently inhibits AngII-dependent atrial fibrosis and subsequent vulnerability to AF induction, by interfering with AngII-signalling on multiple levels. Nitro-fatty acids thus emerge as potential therapeutic agents for AF either by increasing endogenous levels through dietary interventions or as synthetic drugs.

Supplementary material

Supplementary material is available at *Cardiovascular Research* online.

Acknowledgements

We thank Hartwig Wieboldt and Lisa Remane for expert technical assistance.

Conflict of interest: B.A.F. is the scientific founder of Complexa, Inc., which has licensed intellectual property from the University of Pittsburgh. B.A.F. has a COI management plan established by the university. Complexa, Inc. did not support any aspect of the present study and B.A.F. receives no personal or academic research support from Complexa, Inc. The other authors have no potential conflict of interest.

Funding

This work was supported by the Deutsche Forschungsgemeinschaft (KL 2516/1-1 to A.K.; HE 6855/1-1 to J.K.H.; BA 1870/7-1, BA 1870/9-1 and BA 1870/10-1 to S.B.; RU 1876/1-1 and RU 1876/3-1 to V.R.); the Czech Science Foundation (13-40824P to G.A.), the European Regional Development Fund—Project FNUSA-ICRC (No. CZ.1.05/1.1.00/02.0123 to L.K. and A.K.), the Academy of Science Czech Republic (M200041208 to M.P., G.A., H.M., and L.K.), and NIH grants R01-HL058115, R01-HL64937 and P01-HL103455 (B.A.F.); the DZHK (German Centre for Cardiovascular Research)–Hamburg/Kiel/Luebeck, Hamburg, Germany to A.S.

References

1. Camm AJ, Kirchhof P, Lip GY, Schotten U, Savelieva I, Ernst S, Van Gelder IC, Al-Attar N, Hindricks G, Prendergast B, Heidbuchel H, Alfieri O, Angelini A, Atar D, Colonna P, De Caterina R, De Sutter J, Goette A, Gorenek B, Heldal M, Hohloser SH, Kolh P, Le Heuzey JY, Ponikowski P, Rutten FH. Guidelines for the management of atrial fibrillation: the Task Force for the Management of Atrial Fibrillation of the European Society of Cardiology (ESC). *Eur Heart J* 2010;**31**:2369–2429.
2. Burstein B, Nattel S. Atrial fibrosis: mechanisms and clinical relevance in atrial fibrillation. *J Am Coll Cardiol* 2008;**51**:802–809.
3. Kim YM, Guzik TJ, Zhang YH, Zhang MH, Kattach H, Ratnatunga C, Pillai R, Channon KM, Casadei B. A myocardial Nox2 containing NAD(P)H oxidase contributes to oxidative stress in human atrial fibrillation. *Circ Res* 2005;**97**:629–636.
4. Rubbo H, Radi R, Trujillo M, Telleri R, Kalyanaraman B, Barnes S, Kirk M, Freeman BA. Nitric oxide regulation of superoxide and peroxynitrite-dependent lipid peroxidation. Formation of novel nitrogen-containing oxidized lipid derivatives. *J Biol Chem* 1994;**269**:26066–26075.
5. Rudolph V, Schopfer FJ, Khoo NK, Rudolph TK, Cole MP, Woodcock SR, Bonacci G, Groeger AL, Golin-Bisello F, Chen CS, Baker PR, Freeman BA. Nitro-fatty acid metabolome: saturation, desaturation, beta-oxidation, and protein adduction. *J Biol Chem* 2009;**284**:1461–1473.
6. Kansanen E, Jyrkkänen HK, Volger OL, Leinonen H, Kivelä AM, Häkkinen SK, Woodcock SR, Schopfer FJ, Horrevoets AJ, Ylä-Herttuala S, Freeman BA, Levonen AL. Nrf2-dependent and -independent responses to nitro-fatty acids in human endothelial cells: identification of heat shock response as the major pathway activated by nitro-oleic acid. *J Biol Chem* 2009;**284**:33233–33241.
7. Bonacci G, Baker PR, Salvatore SR, Shores D, Khoo NK, Koenitzer JR, Vitturi DA, Woodcock SR, Golin-Bisello F, Cole MP, Watkins S, St Croix C, Batthyany CI, Freeman BA, Schopfer FJ. Conjugated linoleic Acid is a preferential substrate for fatty acid nitration. *J Biol Chem* 2012;**287**:44071–44082.
8. Rudolph V, Andrié RP, Rudolph TK, Friedrichs K, Klinke A, Hirsch-Hoffmann B, Schwoerer AP, Lau D, Fu X, Klingel K, Sydow K, Didié M, Seniuk A, von Leitner EC, Szoecs K, Schrickel JW, Treede H, Wenzel U, Lewalter T, Nickenig G, Zimmermann WH, Meinertz T, Böger RH, Reichenspurner H, Freeman BA, Eschenhagen T, Ehmke H, Hazen SL, Willems S, Baldus S. Myeloperoxidase acts as a profibrotic mediator of atrial fibrillation. *Nat Med* 2010;**16**:470–474.
9. Tarpey MM, Fridovich I. Methods of detection of vascular reactive species: nitric oxide, superoxide, hydrogen peroxide, and peroxynitrite. *Circ Res* 2001;**89**:224–236.
10. Miller FJ, Gutterman DD, Rios CD, Heistad DD, Davidson BL. Superoxide production in vascular smooth muscle contributes to oxidative stress and impaired relaxation in atherosclerosis. *Circ Res* 1998;**82**:1298–1305.
11. Desplantez T, McCain ML, Beauchamp P, Rigoli G, Rothen-Rutishauser B, Parker KK, Kleber AG. Connexin43 ablation in foetal atrial myocytes decreases electrical coupling, partner connexins, and sodium current. *Cardiovasc Res* 2012;**94**:58–65.
12. Tuomi JM, Tyml K, Jones DL. Atrial tachycardia/fibrillation in the connexin 43 G60S mutant (Oculodentodigital dysplasia) mouse. *Am J Physiol Heart Circ Physiol* 2011;**300**:H1402–H1411.
13. Adam O, Lavall D, Theobald K, Hohl M, Grube M, Ameling S, Sussman MA, Rosenkranz S, Kroemer HK, Schäfers H, Böhm M, Laufs U. Rac1-induced connective tissue growth factor regulates connexin 43 and N-cadherin expression in atrial fibrillation. *J Am Coll Cardiol* 2010;**55**:469–480.
14. Boldt A, Wetzel U, Lauschke J, Weigl J, Gummert J, Hindricks G, Kottkamp H, Dhein S. Fibrosis in left atrial tissue of patients with atrial fibrillation with and without underlying mitral valve disease. *Heart* 2004;**90**:400–405.
15. Frustaci A, Chimenti C, Bellocci F, Morgante E, Russo MA, Maseri A. Histological substrate of atrial biopsies in patients with lone atrial fibrillation. *Circulation* 1997;**96**:1180–1184.
16. Xu J, Cui G, Esmailian F, Plunkett M, Marelli D, Ardehali A, Odim J, Laks H, Sen L. Atrial extracellular matrix remodeling and the maintenance of atrial fibrillation. *Circulation* 2004;**109**:363–368.
17. de Jong S, van Veen TA, van Rijen HV, de Bakker JM. Fibrosis and cardiac arrhythmias. *J Cardiovasc Pharmacol* 2011;**57**:630–638.
18. Xie Y, Sato D, Garfinkel A, Qu Z, Weiss JN. So little source, so much sink: requirements for afterdepolarizations to propagate in tissue. *Biophys J* 2010;**99**:1408–1415.
19. Boldt A, Wetzel U, Weigl J, Garbade J, Lauschke J, Hindricks G, Kottkamp H, Gummert JF, Dhein S. Expression of angiotensin II receptors in human left and right atrial tissue in atrial fibrillation with and without underlying mitral valve disease. *J Am Coll Cardiol* 2003;**42**:1785–1792.
20. Tsai CT, Tseng CD, Hwang JJ, Wu CK, Yu CC, Wang YC, Chen WP, Lai LP, Chiang FT, Lin JL. Tachycardia of atrial myocytes induces collagen expression in atrial fibroblasts through transforming growth factor β1. *Cardiovasc Res* 2011;**89**:805–815.
21. Xiao HD, Fuchs S, Campbell DJ, Lewis W, Dudley SC, Kasi VS, Hoit BD, Keshelava G, Zhao H, Capecchi MR, Bernstein KE. Mice with cardiac-restricted angiotensin-converting enzyme (ACE) have atrial enlargement, cardiac arrhythmia, and sudden death. *Am J Pathol* 2004;**165**:1019–1032.
22. Weber KT, Sun Y, Bhattacharya SK, Ahokas RA, Gerling IC. Myofibroblast-mediated mechanisms of pathological remodelling of the heart. *Nat Rev Cardiol* 2012;**10**:15–26.
23. Mihm MJ, Yu F, Carnes CA, Reiser PJ, McCarthy PM, Van Wagoner DR, Bauer JA. Impaired myofibrillar energetics and oxidative injury during human atrial fibrillation. *Circulation* 2001;**104**:174–180.
24. Adam O, Frost G, Custodis F, Sussman MA, Schäfers HJ, Böhm M, Laufs U. Role of Rac1 GTPase activation in atrial fibrillation. *J Am Coll Cardiol* 2007;**50**:359–367.
25. Yamashita T, Sekiguchi A, Iwasaki YK, Date T, Sagara K, Tanabe H, Suma H, Sawada H, Aizawa T. Recruitment of immune cells across atrial endocardium in human atrial fibrillation. *Circ J* 2010;**74**:262–270.

26. Rosen GM, Pou S, Ramos CL, Cohen MS, Britigan BE. Free radicals and phagocytic cells. *FASEB J* 1995;**9**:200–209.
27. Yamamori T, Inanami O, Nagahata H, Cui Y, Kuwabara M. Roles of p38 MAPK, PKC and PI3-K in the signaling pathways of NADPH oxidase activation and phagocytosis in bovine polymorphonuclear leukocytes. *FEBS Lett* 2000;**467**:253–258.
28. Griendling KK, Sorescu D, Lassègue B, Ushio-Fukai M. Modulation of protein kinase activity and gene expression by reactive oxygen species and their role in vascular physiology and pathophysiology. *Arterioscler Thromb Vasc Biol* 2000;**20**:2175–2183.
29. Pepine CJ, Allen HD, Bashore TM, Brinker JA, Cohn LH, Dillon JC, Hillis LD, Klocke FJ, Parmley WW, Ports TA. ACC/AHA guidelines for cardiac catheterization and cardiac catheterization laboratories. American College of Cardiology/American Heart Association Ad Hoc Task Force on Cardiac Catheterization. *Circulation* 1991;**84**:2213–2247.
30. Pekarova M, Lojek A, Martiskova H, Vasicek O, Bino L, Klinke A, Lau D, Kuchta R, Kadlec J, Vrba R, Kubala L. New role for L-arginine in regulation of inducible nitric-oxide-synthase-derived superoxide anion production in raw 264.7 macrophages. *Sci World J* 2011;**11**:2443–2457.
31. Zhang J, Villacorta L, Chang L, Fan Z, Hamblin M, Zhu T, Chen CS, Cole MP, Schopfer FJ, Deng CX, Garcia-Barrio MT, Feng YH, Freeman BA, Chen YE. Nitro-oleic acid inhibits angiotensin II-induced hypertension. *Circ Res* 2010;**107**:540–548.
32. Zografos T, Katritsis DG. Inhibition of the renin-angiotensin system for prevention of atrial fibrillation. *Pacing Clin Electrophysiol* 2010;**33**:1270–1285.